Theoretical analyses on improved beam properties of GaSb-based 2.X-μm quantum-well diode lasers with no degradation in laser parameters*

Wang Yong-Bin(王永宾), Xu Yun(徐 云)†,
Song Guo-Feng(宋国峰), and Chen Liang-Hui(陈良惠)

Laboratory of Nano-Optoelectronics, Institute of Semiconductors, Chinese Academy of Sciences, Beijing 100083, *China*

(Received 20 December 2011; revised manuscript received 17 February 2012)

An asymmetric laser heterostructure is developed to improve the beam properties of GaSb-based diode lasers with no degradation in laser parameters. Employing the semivectorial finite difference method, the dependences of beam divergence and optical confinement factor on waveguide width and refractive index step are investigated theoretically. After carefully design, a particular asymmetric laser structure is proposed. Its beam divergence in the fast axis is reduced from 61° to 34° compared with that of the broad-waveguide structure. The optical confinement factor is approximately equal to 0.0362 and comparable to that of the conventional broad-waveguide structure.

Keywords: broad-waveguide structure, asymmetric heterostructure, beam divergence, optical confinement factor

PACS: 42.55.Px, 42.60.Jf **DOI:** 10.1088/1674-1056/21/8/084208

1. Introduction

GaSb-based quantum-well (QW) lasers emitting around 2 μm (designated as 2.X μm below) have a variety of applications, such as atmospheric pollution monitoring, laser surgery, and optical pump sources for solid-state or fiber lasers. Diode lasers based on a (AlGaIn) (AsSb) material system have been well developed in the past years. High-power lasers with continuous-wave output powers of 1.7 W at 2.0 μm and 0.5 W at 2.7 μm have been achieved.[1−3] A low-threshold laser with a threshold density of 63 $A \cdot cm^{-2}$ per QW at 2.3 μm has been obtained.[4]

Generally, the broadened waveguide (BW) structure is adopted in 2.X μm diode lasers.[5,6] Due to the small overlap between waveguide modes and the highly doped p-cladding layer, the BW structure has the advantage of low internal cavity loss.[7,8] Moreover, it helps to obtain a large equivalent transverse spot size.[9] However, the large optical cavity will result in a large beam divergence in the fast axis of about 63° full width at half maximum (FWHM),[10−12] increasing the difficulties in coupling the light into an optical system efficiently. Nowadays, studies on improving the beam properties of GaSb-based lasers have attracted considerable attention. As reported in previous studies, the beam divergence can be reduced greatly by narrowing the optical waveguide or reducing the refractive index step between the cladding and waveguide layers.[13,14] However, effects of changing these structure parameters on the optical confinement factor in the QWs (Γ_{QW}) have not been taken into account. Favourable reduction of the beam divergence eventually brings on the unfavourable degradation of threshold current and characteristic temperature. A diode laser with the narrowest beam divergence is not at a maximum output power level.[15,16]

In the present paper, we take the conventional BW structure working at 2 μm for example to investigate dependences of optical confinement factor and beam divergence on waveguide width and refractive index step theoretically. A properly designed asymmetric laser structure is obtained, in which both the beam divergence and the favourable optical confinement factor are improved, thus guaranteeing favourable laser performances.

*Project supported by the Beijing Municipal Natural Science Foundation, China (Grant No. 4112058).
†Corresponding author. E-mail: xuyun@red.semi.ac.cn
© 2012 Chinese Physical Society and IOP Publishing Ltd

2. Theoretical model

The popular BW laser emitting at 2 μm is investigated numerically, and its typical device structure is as follows. The active layer consists of three compressively strained 10-nm-thick $Ga_{0.82}In_{0.18}Sb$ QWs, separated by 20-nm-wide lattice matched $Al_{0.3}Ga_{0.7}As_{0.02}Sb_{0.98}$ barriers. The QW region is surrounded by the 400-nm-thick nominally undoped $Al_{0.3}Ga_{0.7}As_{0.02}Sb_{0.98}$ layers, followed by 1.5-μm-thick $Al_{0.9}Ga_{0.1}As_{0.07}Sb_{0.93}$ n-doped and p-doped cladding layers. It should be noted that the stripe width and ridge depth of the device are taken to be 8 μm and 1.2 μm in the following calculations, respectively.

The semivectorial finite difference method (FDM) with nonuniform discretization is employed for the theoretical analysis.[17−19] To simplify the problem, the refractive index in the z direction is taken to be constant. As shown in Fig. 1, the waveguide structure is divided into rectangles along the growth (y) and lateral (x) direction. Variable grid spacings both in x and y directions enable us to calculate a complicated structure with small geometry accurately. Each rectangle is represented by a corresponding cell point, which is right in the centre of each cell. The refractive index in each cell is assumed to be uniform, and the index changes only at cell boundaries.

Based on the semivectorial approximation theory, the components of electric and magnetic fields are functions of x and y only. Thus wave equations for the two-dimensional ridge waveguide can be derived from Maxwell's equations

$$\begin{aligned} \frac{\partial^2 E_x}{\partial x^2} + \frac{\partial^2 E_x}{\partial y^2} + (\tilde{k}^2 - \tilde{\beta}^2)E_x = 0, \\ \frac{\partial^2 E_y}{\partial x^2} + \frac{\partial^2 E_y}{\partial y^2} + (\tilde{k}^2 - \tilde{\beta}^2)E_y = 0, \end{aligned} \tag{1}$$

where $\tilde{k}$ is the complex wavenumber and $\tilde{\beta}$ is the complex propagation constant.

Wave equations at cell point of (x_i, y_j) could be rewritten in the five-point difference form:

$$\begin{aligned} a_{i-1,j}E_{i-1,j} + a_{i+1,j}E_{i+1,j} + a_{i,j-1}E_{i,j-1} \\ + a_{i,j+1}E_{i,j+1} + a_{i,j}E_{i,j} = \tilde{\beta}^2 E_{i,j}. \end{aligned} \tag{2}$$

The sequence of cell subscripts (i, j) increases with x and y increasing, respectively. $E_{i-1,j}$, $E_{i+1,j}$, $E_{i,j-1}$, $E_{i,j+1}$, and $E_{i,j}$ are field amplitudes in corresponding cells; $a_{i-1,s}$, $a_{i+1,s}$, $a_{i,j-1}$, $a_{i,j+1}$, and $a_{i,j}$ are corresponding difference coefficients. For cells at grid boundaries, field amplitudes are assumed to decay exponentially in this calculation.

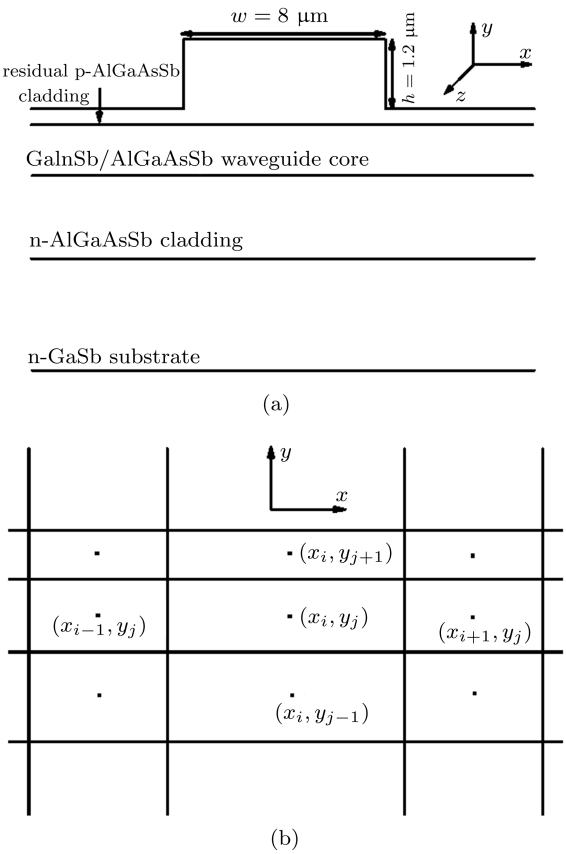


Fig. 1. (a) Two-dimensional ridge waveguide structure of GaSb-based diode laser. The ridge width w and the ridge depth h are 8 μm and 1.2 μm in the following calculations, respectively. The directions of the axes are also shown. (b) Nonuniformly discretized grid for an FDM scheme with a cell point right in the centre of each cell. The number of cells in the x and y directions in the following calculations are 60 and 325, respectively.

The column vector $\tilde{E}$ is composed of all the field amplitudes in different cells, and the square matrix R is composed of their corresponding coefficients. Therefore, equations in the five-point difference form can be converted into the algebraic eigenvalue problem:

$$R\tilde{E} = \tilde{\beta}^2 \tilde{E}. \tag{3}$$

The shifted inverse power iteration method is employed to locate any required propagation eigenvalue and its corresponding electric field profile for the mode under investigation.[20,21] Far-field distributions can be deduced from the field profiles in the following form:[22]

$$\tilde{S}(r, \theta, \varphi) = \frac{4\pi^2}{\omega\mu r^2}(k_z^2 + k_{x,y}^2)\,|A_{x,y}|^2\,\tilde{k}, \tag{4}$$

where $A_{x,y}$ is the Fourier transform of electric fields.

3. Results and discussion

The quasi-TE fundamental mode profile and far field distribution of the BW structure are calculated as shown in Fig. 2. The near-field intensity profile is located mainly in optical confinement layers, and $\Gamma_{\rm QW}$ approximately equals 0.0367. The BW structure has a beam divergence of above 60° full width at half maximum (FWHM) in the fast axis. Such a large divergence requires the optics with a numerical aperture larger than 0.5 for efficient collection of the light produced by diode lasers.

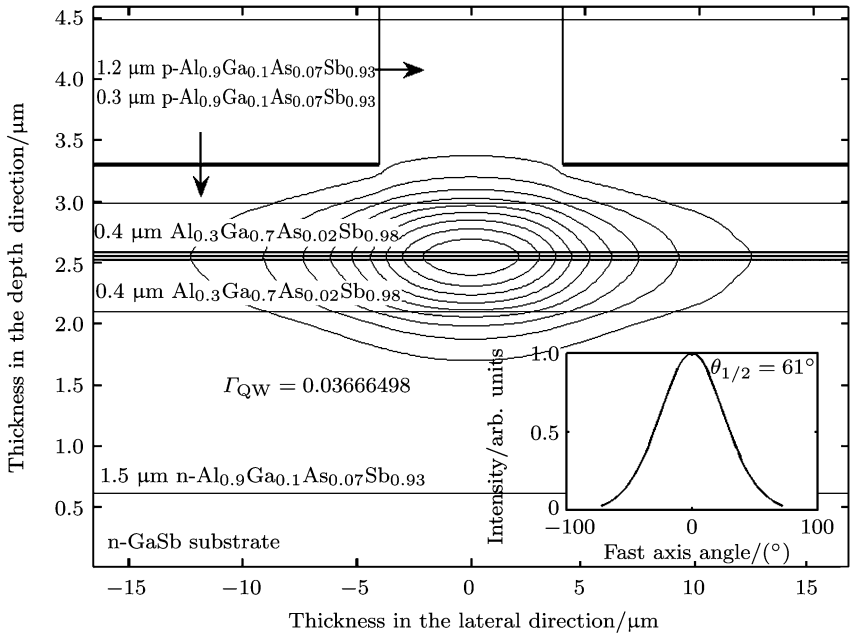


Fig. 2. Calculated intensity profile of quasi-TE fundamental mode for the conventional GaSb-based symmetric BW heterostructure. Inset shows the far field distribution of this structure. The optical confinement factor $\Gamma_{\rm QW}$ and the transverse beam FWHM $\theta_{1/2}$ are calculated.

In order to solve the problem of large beam divergence and maintain the favourable optical confinement factor as well, we investigate their relationships with the waveguide width and refractive index step. As shown in Fig. 3, the FWHM of the beam divergence ($\theta_{1/2}$) below 50° can be obtained from the symmetric heterostructure with waveguide width below 0.3 μm. However, due to the increased overlap between waveguide modes and the highly doped p-cladding, it deteriorates the BW design and thus brings on large internal loss. Besides, large $\Gamma_{\rm QW}$ resulting from narrow waveguide width leads to a small equivalent transverse spot size, which restricts the maximum output power of diode lasers.[23,24] Broadened waveguides with a width of more than 1 μm can improve beam properties of the device as well, but they can cause significant decrease in output efficiency at high currents because of the quasineutral electron–hole plasma accumulating in the optical confinement layers. Furthermore, thick waveguides increases the threshold current of diode lasers due to the deteriorative optical-confinement factor.[25−27] Figure 4 shows that there is a serious modal leakage into highly doped cladding layers due to small refractive index step. The increased refractive index step is helpful for improving active layer confinement factor, but it leads to degraded beam divergence. Therefore a tradeoff between $\theta_{1/2}$ and $\Gamma_{\rm QW}$ must be taken into account in the design of conventional BW laser.

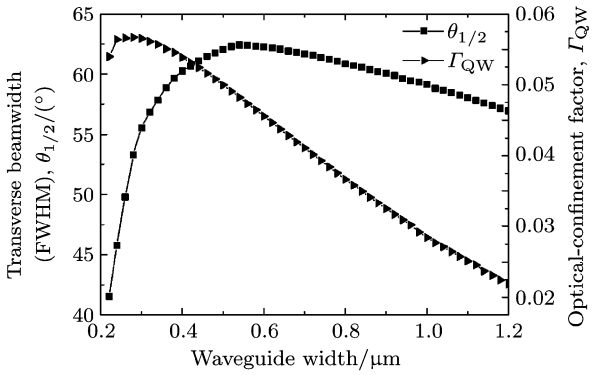


Fig. 3. Theoretical simulations of $\theta_{1/2}$ and $\Gamma_{\rm QW}$ versus the waveguide width for the GaSb-based symmetric BW structure.

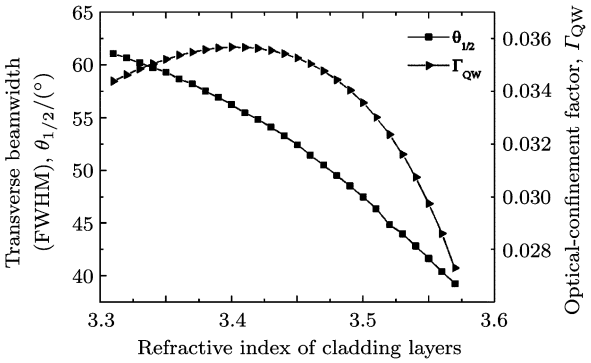


Fig. 4. Theoretical simulations of $\theta_{1/2}$ and $\Gamma_{\rm QW}$ versus the refractive index of cladding layers for the GaSb-based symmetric BW structure, with the corresponding Al-content in quaternary AlGaAsSb cladding layers varying from 90% to 35%. The refractive index of waveguide layers stays unchanged during the simulation.

An asymmetric heterostructure with narrow waveguides is proposed to solve the dilemma. Here we will illustrate that the asymmetric structure is useful for obtaining the favourable optical confinement factor as well as the reduced beam divergence through careful design, thus guaranteeing favourable laser performances. Asymmetric waveguides would spread optical mode selectively into the n-cladding. Hence, there is no substantial increase of the internal loss. Narrow waveguides with width below 300 nm are necessary to obtain low $\theta_{1/2}$ and favourable $\Gamma_{\rm QW}$ (Fig. 3). Asymmetric claddings are also required to further improve beam properties and maintain favourable optical confinement factor. There are several options for refractive indices of asymmetric claddings to meet our requirements (Fig. 5). Therefore, properly designed asymmetric structures provide chances to solve the problem of large beam divergence for GaSb-based diode lasers with no degradation in laser parameters.

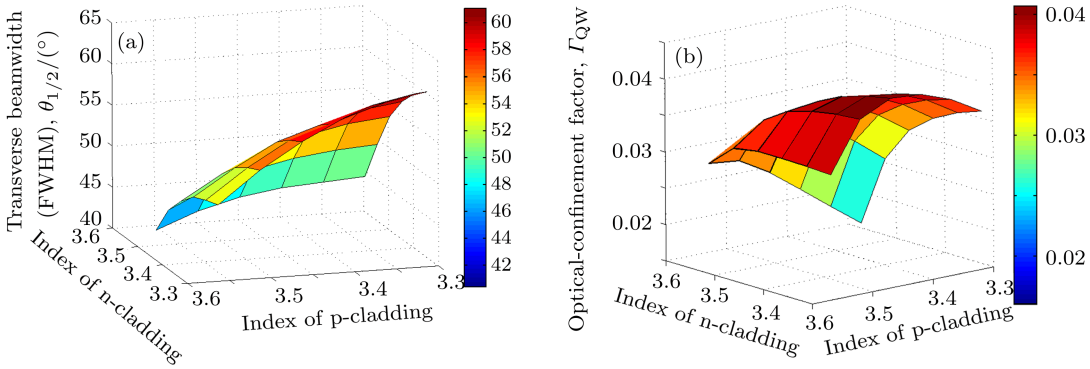


Fig. 5. (colour online) Three-dimensional views of $\theta_{1/2}$ (a) and $\Gamma_{\rm QW}$ (b) versus asymmetric cladding layer for GaSb-based diode laser. Notice that the device structure is the same as the symmetric BW structure except for asymmetric cladding layer. We can clearly see that with properly designed asymmetric cladding, both the low $\theta_{1/2}$ and favourable $\Gamma_{\rm QW}$ can be obtained.

In light of theoretical results calculated above, we discuss a particular asymmetric laser structure. Al-content values in p-type and n-type cladding layers reduce from 90% to 60% and 50%, respectively. Waveguide widths of p-type and n-type layers reduce to 150 nm and 100 nm, respectively. Considering the strong shift of the mode into the n-type cladding, we must increase the n-cladding thickness to prevent the modal intensity from leaking into the high-index GaSb substrate. Therefore, the n-cladding with a thickness of 3.5 μm is employed in the asymmetric structure.

Figure 6 shows the fundamental mode and far field distributions in the asymmetric structure. The modal field is located mainly in the n-cladding layer, so the internal loss from the highly doped p-cladding can be reduced greatly. Besides, the high doping profile in the p-cladding guarantees that there is no penalty in the laser electrical characteristics. By shifting QW active region closer towards the n-cladding, the reduced overlap between mode intensity and waveguide layers is beneficial for the reduction of optical loss induced by free carrier absorption at high currents. The optical confinement actor approximately is equal to 0.0362 and comparable to that of the conventional BW structure. Meanwhile, the FWHM of the far field intensity is reduced.

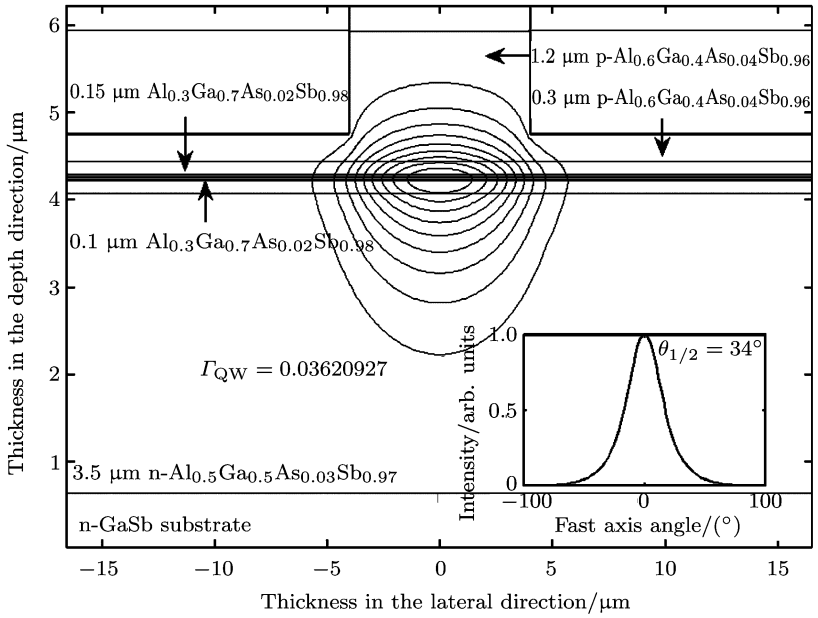


Fig. 6. Calculated intensity profile of quasi-TE fundamental mode for the GaSb-based asymmetric heterostructure with narrow waveguides. Inset shows the far field distribution of this structure.

4. Conclusion

For GaSb-based diode lasers, dependences of $\theta_{1/2}$ and $\Gamma_{\rm QW}$ on the optical waveguide width and refractive index step are investigated theoretically. An asymmetric heterostructure is developed to improve beam properties without any loss in laser performances. After carefully designing the width of the asymmetric waveguides and the refractive indices of the asymmetric claddings, a particular asymmetric laser heterostructure is discussed in detail. The beam divergence in the fast axis is reduced from 61° to 34° FWHM compared with that of the BW structure. Moreover, the optical confinement factors between the two structures are comparable. Therefore, the properly designed asymmetric heterostructure is suitable for GaSb-based diode lasers with favourable laser performances. Conclusions drawn from diode lasers working at 2 μm are also applicable for the other GaSb-based 2.X-μm diode lasers.

References

[1] Garbuzov D, Martinelli R, Lee H, Menna R, York P, Dimarco L, Harvey M, Mararese R, Narayan S and Connolly J 1997 *Appl. Phys. Lett.* **70** 2931

[2] Rattunde M, Mermelstein C, Schmitz J, Kiefer R, Pletschen W, Walther M and Wagner J 2002 *Appl. Phys. Lett.* **80** 4085

[3] Kim J G, Shterengas L, Martinelli R U and Belenky G L 2003 *Appl. Phys. Lett.* **83** 1926

[4] Salhi A, Rouillard Y, Pérona A, Grech P, Garcia M and Sirtori C 2004 *Semicond. Sci. Technol.* **19** 260

[5] Petrescu-Prahova I B, Buda M and Van De Roer T G 1994 *IEICE Trans. Electron.* **E77-C** 1472

[6] Garbuzov D. Z, Abeles J H, Morris N A, Gardner P D, Triano A R, Harvey M G, Gilbert D B and Connolly J C 1996 *Proc. SPIE* **2682** 20

[7] Rattunde M, Schmitz J, Kiefer R and Wagner J 2004 *Appl. Phys. Lett.* **84** 4750

[8] Tong C Z, Niu Z C, Han Q and Wu R H 2005 *Acta Phys. Sin.* **54** 3651 (in Chinese)

[9] Mawst L J, Bhattacharya A, Lopez J, Botez D, Garbuzov D Z, Demarco L, Connolly J C, Jansen M, Fang F and Nabiev R F 1996 *Appl. Phys. Lett.* **69** 1532

[10] Belenky G, Kim J, Shterengas L, Gourevitch A and Martinelli R 2004 *Electron. Lett.* **40** 737

[11] Mermelstein C, Rattunde M, Schmitz J, Simanowski S, Kiefer R, Walther M and Wagner J 2002 *Mater. Res. Soc. Symp. Proc.* **692** 365

[12] Choi H, Turner G, Walpole J, Manfra M and Connors M 1998 *Proc. SPIE* **3284** 268

[13] Ryvkin B S and Avrutin E A 2005 *J. Appl. Phys.* **98** 026107

[14] Rattunde M, Schmitz J, Kaufel G, Kelemen M, Weber J and Wagner J 2006 *Appl. Phys. Lett.* **88** 081115

[15] Chen J F, Kipshidze G and Shterengas L 2010 *IEEE J. Quantum Electron.* **46** 1464

[16] Li Z G, Liu G J, You M H, Li L, Li M, Wang Y, Zhang B S and Wang X H 2009 *Semiconductor Lasers* **19** 1230

[17] Stern M S 1988 *IEE Proc. Pt. J.* **135** 56

[18] Kim C M and Ramaswamy R V 1989 *IEEE J. Lightwave Technology* **1** 1581

[19] Xiao J B, Zhang M D and Sun X H 2006 *Chin. Phys.* **15** 143

[20] Wilkinson J H 1964 *An Introduction to Numerical Linear Algebra* (Oxford: Clarendon Press)

[21] Zhao G Z, Yu X J, Xu Y and Zhu J 2010 *Chin. Phys.* B **19** 070203
[22] Gan Q Q, Zhu X P, Pan X J, Deng J, Song G F and Chen L H 2004 *Laser Technology* **28** 298
[23] Botez D 1999 *Appl. Phys. Lett.* **74** 3102
[24] Lee J J, Mawst L J and Botez D 2002 *IEEE Photon. Technol. Lett.* **14** 1046
[25] Taylor G W and Claisse P R 1995 *IEEE J. Quantum Electron.* **31** 2133
[26] Asryan L V, Luryi S and Suris R A 2003 *IEEE J. Quantum Electron.* **39** 404
[27] Belenky G, Shterengas L, Wang D, Kipshidze G and Vorobjev L 2009 *Semicond. Sci. Technol.* **24** 115013